OPEN ACCESS



S₈ Tension in the Context of Dark Matter–Baryon Scattering

Adam He¹, Mikhail M. Ivanov^{2,3,4}, Rui An¹, and Vera Gluscevic¹
Department of Physics and Astronomy, University of Southern California, Los Angeles, CA 90089, USA; adamhe@usc.edu
² School of Natural Sciences, Institute for Advanced Study, 1 Einstein Drive, Princeton, NJ 08540, USA
³ Center for Theoretical Physics, Massachusetts Institute of Technology, Cambridge, MA 02139, USA

**Received 2023 April 6; revised 2023 May 29; accepted 2023 June 4; published 2023 August 29

Abstract

We explore an interacting dark matter (IDM) model that allows for a fraction of dark matter (DM) to undergo velocity-independent scattering with baryons. In this scenario, structure on small scales is suppressed relative to the cold DM scenario. Using the effective field theory of large-scale structure, we perform the first systematic analysis of BOSS full-shape galaxy clustering data for the IDM scenario, and we find that this model ameliorates the S_8 tension between large-scale structure and Planck data. Adding the S_8 prior from the Dark Energy Survey (DES) to our analysis further leads to a mild $\sim 3\sigma$ preference for a nonvanishing DM-baryon scattering cross section, assuming $\sim 10\%$ of DM is interacting and has a particle mass of 1 MeV. This result produces a modest $\sim 20\%$ suppression of the linear power at $k \lesssim 1 h \, \text{Mpc}^{-1}$, consistent with other small-scale structure observations. Similar scale-dependent power suppression was previously shown to have the potential to resolve S_8 tension between cosmological data sets. The validity of the specific IDM model explored here will be critically tested with upcoming galaxy surveys at the interaction level needed to alleviate the S_8 tension.

Unified Astronomy Thesaurus concepts: Dark matter (353); Cosmology (343); Particle astrophysics (96); Redshift surveys (1378); Cosmic microwave background radiation (322); Large-scale structure of the universe (902)

1. Introduction

An abundance of cosmological and astrophysical observations suggests that the majority of matter in the universe is non-baryonic dark matter (DM; Bertone et al. 2005). The current leading Λ CDM cosmological model posits that DM is cold and collisionless and has held up well in light of cosmological data. However, there are tensions between cosmological parameters inferred from the early- and late-universe probes under the Λ CDM model (Abdalla et al. 2022), which could be a consequence of unknown systematic errors (Bernal et al. 2016; Valentino et al. 2021a) or an indication of new physics beyond Λ CDM (Valentino et al. 2021b; Abdalla et al. 2022).

In particular, the S_8 tension at the 2.5σ level is now established between large-scale structure (LSS) data and the cosmic microwave background (CMB) anisotropy measurements from Planck, and recent studies have shown that scaledependent suppression of the linear matter power spectrum might be able to resolve the S_8 tension. Such suppression can occur as a result of baryonic physics (Amon & Efstathiou 2022), or it may arise from new physics associated with dark energy and DM (Poulin et al. 2023). In this study, we consider a scenario where scale-dependent suppression of matter clustering occurs as a result of elastic collisions between a fraction of DM and baryons (Boddy et al. 2018). Such a scenario arises in compelling DM models, including the weakly interacting massive particles (WIMPs) and a whole landscape of new interacting DM (IDM) scenarios, and has been extensively studied and constrained with direct detection and cosmological probes (Sigurdson et al. 2004; Boehm & Schaeffer 2005;

Original content from this work may be used under the terms of the Creative Commons Attribution 4.0 licence. Any further distribution of this work must maintain attribution to the author(s) and the title of the work, journal citation and DOI.

Cushman et al. 2013; Dvorkin et al. 2014; Battaglieri et al. 2017; Boddy & Gluscevic 2018; Boddy et al. 2018; Gluscevic & Boddy 2018; Slatyer & Wu 2018; Gluscevic et al. 2019; Nadler et al. 2019; Becker et al. 2021; Maamari et al. 2021; Nadler et al. 2021; Nguyen et al. 2021; Xu & Farrar 2021; Akerib et al. 2022; Buen-Abad et al. 2022; Hooper et al. 2022; Li et al. 2023; Rogers et al. 2022).

In IDM cosmology, DM exchanges heat and momentum with baryons, and matter perturbations experience collisional damping, leading to a scale-dependent suppression of structure (Bœhm et al. 2001; Boehm & Schaeffer 2005) illustrated in Figure 1. Galaxy clustering and lensing have not previously been used for parameter inference in IDM cosmology. At the same time, the best-fit value of S_8 shifts in the presence of IDM (Gluscevic & Boddy 2018), even when the linear cosmology is considered, including the CMB measurements from Planck (Boddy et al. 2018; Nguyen et al. 2021) and the Ly α forest data (Becker et al. 2021; Hooper et al. 2022; Rogers et al. 2022). In this study, we derive the first bounds on the DM-baryon elastic scattering cross section from galaxy clustering measured in the Baryon Oscillation Spectroscopic Survey (BOSS; Alam et al. 2017), with and without the S_8 prior derived from the Dark Energy Survey data (Abbott et al. 2022). In particular, we consider elastic scattering between DM and protons³ and its effect on the S_8 tension between the early- and late-universe measurements of structure.

In addition to linear cosmology, the population statistic of the satellite galaxies in the Milky Way (MW) place stringent observational bounds on IDM (Nadler et al. 2021). Taking both Ly α forest measurements and Milky Way satellite measurements into account, the suppression of power in the range of scales corresponding to wavenumbers $0.2 \lesssim k \lesssim 2 \, h \, {\rm Mpc}^{-1}$ is only allowed up to 25% (Chabanier et al. 2019; Nadler et al. 2021).

⁴ NASA Hubble Fellowship Program Einstein Postdoctoral Fellow.

⁵ The correction arising from the presence of helium and other light elements is negligible, as shown in previous studies (Boddy et al. 2018). We therefore use "protons" and "baryons" interchangeably here.

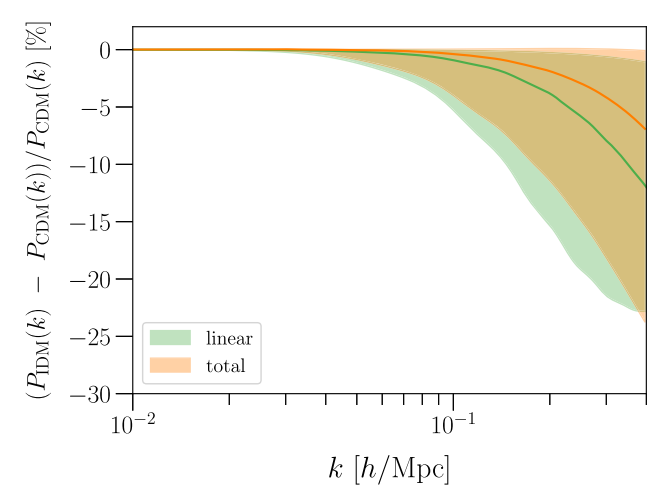


Figure 1. Percent difference between the matter power spectrum for an IDM cosmology with DM-baryon scattering and collisionless cold DM (CDM) cosmology. The linear power spectrum is shown in green, and the total power spectrum is shown in orange. The lines are generated with the best-fit parameter values from a joint Planck + BOSS + the Dark Energy Survey (DES) analysis of the IDM model with a DM mass of 1 MeV and interacting fraction $f_\chi = 10\%$. The shaded bands designate the uncertainty in reconstructed matter power spectrum that corresponds to a 1σ uncertainty around these best-fit parameter values. An increase in the interaction cross section and in the interacting fraction leads to a greater suppression in P(k), while the former also shifts the onset of suppression to larger scales.

Interestingly, beyond- Λ CDM models that alleviate S_8 tension tend to feature a specific form of the scale-dependent suppression in the linear transfer function. In particular, results in Amon & Efstathiou (2022), Preston et al. (2023) show a preference for a power-suppression plateau at small scales, inferred from a joint analysis of the weak-lensing survey data and the CMB anisotropy. In the context of IDM, $\sim 10\%$ fractional cases also produce suppression of this form, while larger fractions gradually depart from the plateau feature (Figure 2). For this reason, we focus on scenarios where 5%-15% of DM interacts with baryons, and undergoes collisional damping, while the rest of DM is collisionless. These cases are consistent with the bounds from the Milky Way satellite abundance and the Ly α forest data. The linear matter power spectrum P(k) and its nonlinear corrections are illustrated in Figure 1.

In addition, direct detection constraints severely limit interactions for heavy DM particles, so we focus on sub-GeV DM candidates only (Angle et al. 2008; Aalseth et al. 2013; Angloher et al. 2016; Agnese et al. 2016; Akerib et al. 2017; Amole et al. 2017; Angloher et al. 2017; Kim et al. 2017; Agnese et al. 2018; Agnese et al. 2018; Aprile et al. 2018; Aguilar-Arevalo et al. 2019; Amole et al. 2019). Our analysis considers the simplest scenario where velocity-independent and spin-independent scattering occurs between DM and protons; we leave a complete consideration of velocity-dependent scattering for future work.

We find that the velocity-independent DM-baryon scattering with 10% of DM allowed to scatter with baryons is consistent with both BOSS and Planck data and ameliorates the S_8 tension between LSS and CMB data. After combining BOSS and Planck with weak-lensing measurements from the Dark Energy Survey, there is a $\sim 3\sigma$ preference for a nonzero interaction cross section at multiple DM particle masses. While the preference is mild, it is also consistent with all known observational bounds on DM interaction physics and warrants

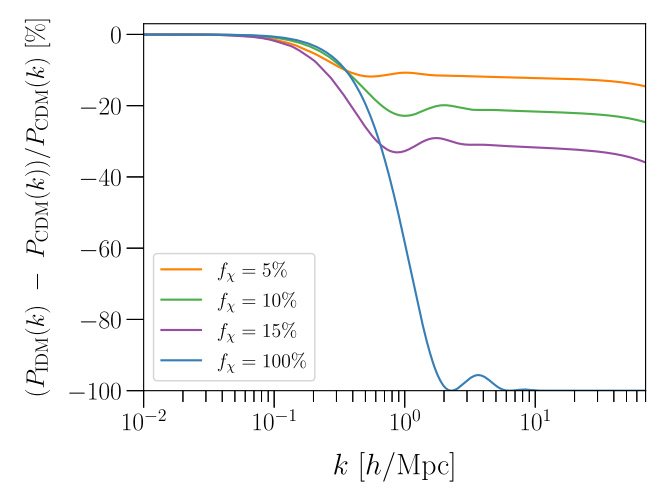


Figure 2. Effect of varying the IDM fraction f_{χ} on the linear matter power spectrum for a cosmology with DM-baryon scattering. The residuals of the linear spectra w.r.t. CDM are shown for $f_{\chi} = 5\%$, 10%, 15%, and 100%. These spectra are generated with the best-fit parameter values from a joint Planck + BOSS + DES analysis of each fraction for a DM mass of $m_{\chi} = 1$ MeV. Fractions higher than $\sim 10\%$ generate a strong power suppression in the range $0.2 \lesssim k \lesssim 2~h~{\rm Mpc}^{-1}$ for this choice of cross section and are thus ruled out by Ly α forest and Milky Way satellite data.

further consideration. In particular, the preferred range of nonzero scattering cross sections can be critically tested in the coming decade with a wide variety of small-scale structure probes, including the $Ly\alpha$ measurements from the Dark Energy Spectroscopic Instrument (DESI; Aghamousa et al. 2016) and the census of dwarf galaxies from the Vera C. Rubin Observatory (Ivezić et al. 2019). More generally, our results are indicative of the preference toward the scale-dependent power suppression that helps to reconcile cosmological data sets; this suppression of power is of similar nature to that seen in other proposed solutions to S_8 tension in the literature (Ye et al. 2021; Amon & Efstathiou 2022; Poulin et al. 2023).

This Letter is organized as follows. In Section 2, we briefly describe the cosmology of IDM, and in Section 3, we outline our methods. Section 4 presents the key results of our data analysis. We discuss and conclude in Section 5.

2. Matter Perturbations in IDM

Within an IDM cosmology that features elastic scattering between DM and baryons, the linear Boltzmann equations contain interaction terms that capture momentum transfer between the two cosmological fluids (Boddy et al. 2018; Gluscevic & Boddy 2018),

$$\dot{\delta}_{\chi} = -\theta_{\chi} - \frac{\dot{h}}{2}, \qquad \dot{\delta}_{b} = -\theta_{b} - \frac{\dot{h}}{2},
\dot{\theta}_{\chi} = -\frac{\dot{a}}{a}\theta_{\chi} + c_{\chi}^{2}k^{2}\delta_{\chi} + R_{\chi}(\theta_{b} - \theta_{\chi}),
\dot{\theta}_{b} = -\frac{\dot{a}}{a}\theta_{b} + c_{b}^{2}k^{2}\delta_{b} + \frac{\rho_{\chi}}{\rho_{b}}R_{\chi}(\theta_{\chi} - \theta_{b})
+ R_{\gamma}(\theta_{\gamma} - \theta_{b}), \tag{1}$$

where subscripts χ and b denote DM and baryons, respectively. δ denotes density perturbations, θ represents velocity divergence; h is the trace of the scalar metric perturbation; c represents the sound speeds in respective fluids; R_{γ} is the momentum transfer rate between baryons and photons from

Compton scattering; and R_{χ} is the momentum transfer rate between DM and baryons from their nongravitational interaction,

$$R_{\chi} = \frac{1}{3} \sqrt{\frac{2^{7}}{\pi}} \frac{a\rho_{b}\sigma_{0}}{m_{\chi} + m_{b}} \left(\frac{T_{\chi}}{m_{\chi}} + \frac{T_{b}}{m_{b}} + \frac{V_{\text{RMS}}^{2}}{3} \right)^{-\frac{1}{2}}, \tag{2}$$

where m_{χ} is the DM particle mass, m_b is the mean baryon mass, and T denotes fluid temperatures. The rms bulk relative velocity between DM and baryons is defined as (Dvorkin et al. 2014)

$$V_{\rm RMS}^2 = \langle \vec{V}_{\chi}^2 \rangle_{\xi} = \int \frac{dk}{k} \Delta_{\xi} \left(\frac{\theta_{\rm b} - \theta_{\chi}}{k^2} \right)^2, \tag{3}$$

where Δ_{ξ} is the primordial curvature variance per log wavenumber k. An integral over k appearing in the Boltzmann equations introduces mode mixing; however, an analytic approximation for the bulk relative velocity that remains constant for $z>10^3$ and scales linearly with z for $z\lesssim 10^3$ is used to reproduce the effect of $V_{\rm RMS}^2$ on R_{χ} with a precision adequate for cosmological analyses (Tseliakhovich & Hirata 2010; Dvorkin et al. 2014; Boddy et al. 2018; Gluscevic & Boddy 2018). To solve the Boltzmann equations in the presence of IDM, we use a modified version of the Boltzmann solver CLASS, which allows for DM-baryon scattering parameterized by a momentum transfer cross section σ_0 (Boddy et al. 2018; Gluscevic & Boddy 2018).

In order to make a prediction for late-time evolution of the matter power spectrum on scales corresponding to galaxy clustering, weak lensing, and related LSS observables, we merge the modified IDM CLASS code with a CLASS-PT module, previously developed as a tool for the computation of LSS power spectra in the mildly nonlinear regime (Baumann et al. 2012; Carrasco et al. 2012; Cabass et al. 2023; Ivanov 2022). CLASS-PT is a nonlinear perturbation theory extension of CLASS that calculates nonlinear 1-loop corrections to the linear matter power spectrum and outputs the redshift-space galaxy power spectrum (Chudaykin et al. 2020).

The formalism implemented in CLASS-PT rests on the effective field theory (EFT) of LSS, which should, in principle, be modified in the presence of nongravitational interactions between baryons and DM. However, in the case of velocity-independent interaction, DM-baryon scattering only affects the evolution of matter perturbations at very high redshifts, where nonlinear effects are entirely negligible. At all redshifts relevant to galaxy surveys, the DM-baryon interactions are effectively frozen, and the evolution of structure proceeds as in Λ CDM, with a suppressed initial power spectrum, shown in Figure 1.9 This means the standard implementation of CLASS-PT is

entirely applicable to predicting late-time LSS observables in our scenario of interest.

3. Data and Analysis Methods

We analyze the full Planck 2018 TT, TE, EE, and lensing power spectra (Aghanim et al. 2020a), along with anisotropic galaxy clustering data from BOSS DR12 at z = 0.38 and 0.61 (Alam et al. 2017; Ivanov et al. 2020b, 2020c, see also Chen et al. 2022; Zhang et al. 2022). As in Chudaykin et al. (2021) and Philcox & Ivanov (2022), our analysis is performed up to $k_{\text{max}} = 0.2 \, h/\text{Mpc}$ for the galaxy power spectrum multipoles, from $0.2 < k < 0.4 \ h \, \text{Mpc}^{-1}$ for the real-space power spectrum proxy Q_0 (Ivanov et al. 2022b), and up to $k_{\text{max}} = 0.08 \, h \, \text{Mpc}^{-1}$ for the bispectrum monopole (Ivanov et al. 2022a; Philcox & Ivanov 2022). 10 We also add the post-reconstructed BOSS DR12 BAO data to this data set following Philcox et al. (2020). We stress that our EFT-based full-shape analysis is quite conservative as we consistently marginalize over all necessary nuisance parameters that capture galaxy bias, baryonic feedback, nonlinear redshift-space distortions (RSD), etc. (Philcox & Ivanov 2022). Thus, our analysis is agnostic about the details of galaxy formation. Note that we fit the BOSS galaxy clustering data within the IDM scenario in a fully consistent and rigorous manner, without any hidden ACDM assumptions. This can be contrasted with the standard "compressed" BOSS likelihood consisting of the baryon acoustic oscillation (BAO) and RSD parameters that are derived assuming a fixed Planck-like ΛCDM template for the underlying linear matter power spectrum (Ivanov et al. 2020b; Alam et al. 2021). Moreover, our EFT-based likelihood includes the galaxy power spectrum shape information that is missing in the standard BOSS likelihood (Alam et al. 2017); see Ivanov et al. (2020b) for a detailed discussion.

We also include weak-lensing data from Year 3 of the Dark Energy Survey (DES-Y3), and we argue that the full DES-Y3 likelihood for DM-baryon interactions can be captured with a simple prior: $S_8 = 0.776 \pm 0.017$. This is because S_8 is measured by DES to be the same value for Λ CDM, WDM, and ACDM extensions like early dark energy, indicating a robustness under different cosmological models (Ivanov et al. 2020a; Hill et al. 2020; Abbott et al. 2022; DES Collaboration et al. 2023), as long as the late-time growth of structure is not modified in these models. Also, S_8 is close to being model independent as it is the primary directly observed principle component of the weak-lensing data. In future work, the full DES-Y3 likelihood for DM-baryon scattering should be calculated to confirm our argument; in the meantime, we will treat a prior on S_8 as equivalent to adding the complete DES-Y3 data set to our analysis.

We use the Planck, BOSS, and DES data sets as proxies to data that drive the S_8 tension. We do not consider weak lensing from KiDS-1000 or Hyper Suprime-Cam Year 3 (HSC-Y3) data because their joint analysis with DES-Y3 necessitates modeling of the full covariance (Amon et al. 2022a), which is

⁶ This model of relative bulk velocity is an approximation, and we make this choice for concreteness only; the value of relative bulk velocity does not have an observable effect in the context of velocity-independent DM scattering.

⁷ We note that this model corresponds to the power-law parameterization of the momentum transfer cross section, $\sigma_{\rm MT} = \sigma_0 v^n$, for n=0, previously used in the literature (Dvorkin et al. 2014; Boddy et al. 2018; Gluscevic & Boddy 2018).

https://github.com/Michalychforever/CLASS-PT

⁹ We show that DM-baryon interactions only impact the evolution of matter perturbations at redshifts before recombination in Appendix A.

¹⁰ Our BOSS full-shape likelihood for CLASS-PT is publicly available at https://github.com/oliverphilcox/full_shape_likelihoods.

¹¹ Note that the priors used in our likelihood are significantly wider than the ones chosen in the EFT-based full-shape analysis of Zhang et al. (2022). Our choice ensures that our main cosmological results are independent of priors on nuisance parameters. Note also that in contrast to Zhang et al. (2022), our priors are motivated by the physics of BOSS red luminous galaxies; see Chudaykin et al. (2021) for more details.

beyond the scope of analyses done in this work. We do not include Pantheon+ data (Brout et al. 2022) because this data would only further constrain Ω_m ; since Ω_m is not appreciably correlated with σ_0 , we do not expect this data to alter our results in a significant way. We have checked that the inclusion of eBOSS DR16 BAO does not strengthen our constraints either. Work is underway to convert eBOSS DR16 into a full-shape likelihood and to incorporate Ly α data into our analysis (see, e.g., Ivanov 2021; Chudaykin & Ivanov 2023). Preliminary reports on the suppression on the growth in these data sets (e.g., Ivanov 2021; Goldstein et al. 2023; and references therein) suggest that they may further favor IDM, but future studies are necessary to confirm this expectation.

To obtain bounds on our IDM model for parameters of interest, such as H_0 , S_8 , and the momentum transfer cross section σ_0 , we perform Markov Chain Monte Carlo (MCMC) parameter estimation using our merged CLASS code. We use the MCMC sampler MontePython and interface it with our version of CLASS (Audren et al. 2013; Brinckmann & Lesgourgues 2019). We choose the Metropolis-Hastings algorithm and assume flat priors on $\{\omega_b, \omega_{DM}, 100\theta_s, \tau_{reio}, \omega_{DM}, \tau_{reio}, \omega_{DM}, \omega_{DM}$ $\ln(10^{10}A_{\rm s}), n_{\rm s}\} + \sigma_0$. Following Gluscevic & Boddy (2018), we fix the IDM particle mass m_{χ} in each MCMC fit and consider the following benchmark particle masses: 100 keV, 1 MeV, 20 MeV, and 100 MeV. We choose this mass range because of the strict constraints on IDM from direct detection above 1 GeV, and constraints on $N_{\rm eff}$ that rule out masses lower than ~1 MeV (Lewin & Smith 1996; An et al. 2022). We set the fraction of DM that interacts with baryons f_{y} to be 10%, while the rest of the DM behaves as CDM; then, we perturb the parameter space slightly and explore fractions $f_x = 5\%$, 7.5%, 12.5%, and 15%. We model free-streaming neutrinos as two massless species and one massive species for which $m_{\nu} = 0.06 \, \text{eV}$, in line with the Planck convention (Aghanim et al. 2020c). A chain is deemed converged if the Gelman–Rubin convergence criterion |R-1|is less than 0.01.

4. Results

We find that for all masses tested in the range [0.1, 100] MeV, our model ameliorates the standard S_8 tension between Planck and DES by 30%, decreasing it from 2.6σ to 1.8σ , while leaving the H_0 tension unchanged. When Planck is combined with BOSS, our model reduces the S_8 tension with DES from 2.6σ to 1.3σ . Since the qualitative picture is the same for all models considered, we choose the $m_\chi=1$ MeV case as a baseline. Our results for the $m_\chi=1$ MeV, $f_\chi=10\%$ model are shown in Figure 3, which displays 1D and 2D marginalized posterior distributions for relevant parameters in our analysis, compared to standard results under Λ CDM. We note that our IDM model does not impact $\Omega_{\rm m}$; our model only affects perturbations and not background quantities, which is why Ω_m is indistinguishable from its value in Λ CDM.

Note the strong degeneracy between σ_0 and S_8 . This degeneracy is unsurprising: a higher cross section means that DM and baryons are more strongly coupled, leading to a greater suppression in the power spectrum and a corresponding decrease in S_8 . Therefore, imposing a prior on S_8 that favors

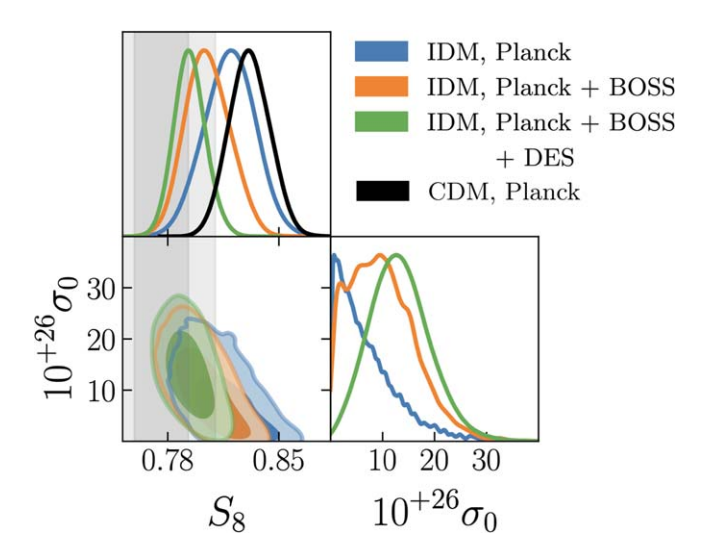


Figure 3. 68% and 95% confidence-level marginalized posterior distributions of relevant parameters for Λ CDM from Planck (black) and our fractional DM–baryon interacting model (colored) from different combinations of Planck, BOSS, and DES data. The gray bands show the DES measurement of S_8 . The bottom right-hand panel shows a 2.6σ preference for nonzero interactions between DM and baryons under a combined Planck, BOSS, and DES analysis.

Model	ΛCDM, Planck + BOSS + DES	IDM, Planck + BOSS + DES
$\sigma_0 (10^{-26} \text{cm}^2)$		13.23 (5.163) ^{+5.2} _{-6.5}
$\Omega_{\rm m}$	$0.308 (0.307) \pm 0.005$	$0.311(0.309) \pm 0.005$
σ_8	$0.802 (0.806) \pm 0.005$	$0.780 \ (0.792)^{+0.007}_{-0.009}$
S_8	$0.813\ (0.815) \pm 0.009$	$0.794 \ (0.804)^{+0.009}_{-0.01}$
$\Delta \chi^2_{ m min}$		-6.7

Note. The maximum of the marginalized posterior (the maximum of the full posterior) and $\pm 68\%$ confidence level uncertainties for cosmological parameters of interest under a Planck + BOSS + DES analysis of our fractional IDM model with a flat prior on σ_0 , compared to Λ CDM. The last row shows the difference in χ^2 with respect to Λ CDM. All IDM values are for $m_\chi = 1$ MeV, $f_\chi = 10\%$.

lower values leads to a mild preference for larger cross sections. Indeed, we observe this in Figure 3: BOSS data prefer a lower value of S_8 as compared to Planck (Philcox & Ivanov 2022), so the combination of Planck and BOSS shifts the σ_0 posterior toward larger cross sections (shown in orange). The combination of Planck and BOSS data with the S_8 prior from DES further disfavors low cross sections, resulting in a preference for nonzero interactions between DM and baryons (shown in green). Overall, Figure 3 shows that the marginalized posterior from a combined Planck + BOSS + DES analysis is maximized for σ_0 value of $1.32^{+0.52}_{-0.65} \times 10^{-25}$ cm² (at 68% confidence level).

In Table 1, we show the values of the relevant parameters that maximize the marginalized posterior and the full posterior (the latter referred to as the best fit), obtained from a Planck + BOSS + DES analysis of the $f_{\chi} = 10\%$, $m_{\chi} = 1$ MeV model, as

 $^{^{12}}$ Following related studies of S_8 tension, we chose a flat prior on σ_0 , and we discuss prior dependence of our results in Appendix E. As expected, a log-flat prior still results in a mild preference for interactions.

well as the χ^2 statistics. We present the full list of constraints on all cosmological parameters for this scenario in Appendix B, and for completeness we show full posterior distributions for this model in Appendix D. The $f_\chi=10\%$, $m_\chi=1$ MeV IDM model, and Λ CDM present similar χ^2 values when analyzed under Planck only; however, we find $\Delta\chi^2=-3.48$ once we include BOSS data, and $\Delta\chi^2=-6.7$ once we include the DES prior on S_8 , corresponding to a 2.6σ preference for nonzero interactions. We note that the preference for nonzero DM-baryon interactions is present even in the BOSS data alone: the IDM fit that contains a single additional free parameter reduces χ^2 by 3.02, compared to the CDM model. We find that our fractional IDM model shows a consistent preference over CDM, regardless of the DM interacting fraction tested; this is discussed further in Appendix C.

5. Summary and Discussion

We considered the concordance of cosmological data in the presence of velocity-independent scattering of baryons with sub-GeV DM particles in the early universe, for scenarios where the interacting component constitutes only a fraction of the total DM abundance. We found that this model is consistent with both the BOSS and Planck data and ameliorates the S_8 tension between LSS and the CMB. After combining BOSS and Planck with the DES weak-lensing prior, we find a 2.6σ preference for nonzero interaction cross section, for a range of DM particle masses and for an interacting fraction $\sim 10\%$.

Our results have implications for DM searches and cosmology in general. Importantly, the model for DM interactions we considered here is quite broad and encompasses a number of well-motivated UV-complete scenarios where DM scatters with normal matter through a heavy mediator exchange at low energies, similar to the WIMP-like scenarios sought in direct detection (Cushman et al. 2013; Gluscevic & Peter 2014). In fact, the scattering interactions that would trigger direct detection (at DM masses above 1 GeV) would also lead to momentum transfer with cosmological consequences, explored here for sub-GeV particles. This study is thus directly complementary to direct detection as it explores different DM mass and cross-section regimes.

The preference we find for nonzero interaction cross section when combining data from Planck, BOSS, and DES implies a preference for scale-dependent suppression in the linear matter power spectrum, similar to that seen in other beyond-CDM models that alleviate the S_8 tension (Ye et al. 2021; Amon & Efstathiou 2022; Poulin et al. 2023). Our expectation is that scale dependence is the primary driver of this preference, for the following reasons. First, the CMB and LSS in general probe different scales (Amon & Efstathiou 2022; Rogers et al. 2023); we note that the CMB lensing has contributions from low redshifts (z < 1), and yet its measurements of S_8 are consistent with those derived from the primary CMB anisotropy (Aghanim et al. 2020b; Qu et al. 2023), consistent with our expectation. Furthermore, IDM only affects matter perturbations long before recombination (Gluscevic & Boddy 2018), acting to ameliorate the tension through scale dependence of the linear power spectrum, rather than modifying clustering of matter at later times. Indeed, Amon & Efstathiou (2022) and Preston et al. (2023) showed that the tension can be framed as a preference for a specific k dependence of the transfer function, which happens to match the fractional IDM case, as discussed in our work; see Figure 2.

While the preference we find is mild and could be a result of a random statistical fluctuation or of an unknown systematic effect (Leauthaud et al. 2017; Amon et al. 2022b; Chaves-Montero et al. 2023), the specific model we consider here has several qualities that set it apart from models that were considered previously in the same context. First, it does not exacerbate the H_0 tension, which is a common drawback of many models proposed to resolve the S_8 tension (Abdalla et al. 2022). Furthermore, it is simple and generic, relying on DM interaction physics that was proposed independent of the status of cosmological concordance.

On the other hand, we wish to point out that the interpretation of the S_8 tension in the context of IDM has the same caveat as most beyond-ΛCDM models considered for the same purpose, in that it features more degrees of freedom than a vanilla cosmology. Namely, this study focused on exploring DM interactions that produce power suppression of the form preferred by the combination of cosmological data which alleviate the S_8 tension; we thus only varied the interaction cross section, while setting f_{χ} and m_{χ} to fixed values. While concrete UV-complete models for DM may not allow the freedom in choosing the fraction and the particle mass, for the effective description of the interaction and for cosmological purposes, these two parameters could be treated as additional degrees of freedom of a larger class of models that produce velocity-independent scattering at low energies. Within that context, a full model-selection exercise should be performed to assess whether data favor IDM or a vanilla cosmology. However, this analysis exceeds the scope of the present work.

The preferred range of interaction cross sections and the corresponding level of power suppression in the linear matter power spectrum we consider here are consistent with all current observations (Xu et al. 2018; Nadler et al. 2019, 2019; Becker et al. 2021; Maamari et al. 2021; Nadler et al. 2021, 2021; Hooper et al. 2022; Rogers et al. 2022). Interestingly, the census of the MW satellite galaxies allows for up to $\sim 25\%-30\%$ decrement in power at $k \sim 30 \, h \, \mathrm{Mpc}^{-1}$, as compared to CDM (Nadler et al. 2019, 2021); this means that small-scale structure probes are on the verge of being able to detect the IDM signal necessary to resolve the tension, likely to be achieved within the next decade. We note that even the combined analyses of the existing measurements from eBOSS (Alam et al. 2021), KiDS (Asgari et al. 2021), and HSC (Hikage et al. 2019) may be able to put further pressure on this model. Beyond the existing data, the matter power spectrum on quasi-linear and nonlinear scales will be measured at high precision with upcoming surveys from DESI, Euclid (Chudaykin & Ivanov 2019; Sailer et al. 2021), and the Vera C. Rubin Observatory (Drlica-Wagner et al. 2019; Nadler et al. 2019). In addition, Stage-3 and Stage-4 data that target high-resolution measurements of the CMB, including the third generation of the South Pole Telescope (SPT-3G; Benson et al. 2014), the Atacama Cosmology Telescope (ACT; Aiola et al. 2020), the Simons Observatory (Ade et al. 2019), CMB-S4 (Abazajian et al. 2016), and CMB-HD (Aiola et al. 2022) will probe quasi-linear scales, providing a longer lever arm for testing details of the scale dependence in the linear matter power spectrum. This study and the recent analyses of the S_8 tension (e.g.,

Amon & Efstathiou 2022; Poulin et al. 2023; Preston et al. 2023; Rogers et al. 2023) highlight the need to further explore predictive models that affect the distribution of matter in the universe.

Acknowledgments

We thank the anonymous referee for their suggestions and careful review of our Letter. We gratefully acknowledge the support from explore.org and Sylvie and David Shapiro at USC. We thank Ethan O. Nadler for providing valuable comments on the manuscript. The work of M.M.I. has been supported by NASA through the NASA Hubble Fellowship grant #HST-HF2-51483.001-A awarded by the Space Telescope Science Institute, which is operated by the Association of Universities for Research in Astronomy, Incorporated, under NASA contract NAS5-26555. R.A. and V.G. acknowledge the support from NASA through the Astrophysics Theory Program, Award No. 21-ATP21-0135. VG acknowledges the support from the National Science Foundation (NSF) CAREER Grant No. PHY-2239205.

Appendix A Evolution of Structure at Low Redshifts

We verify that there are no alternations in structure evolution on *any* wavelength modes after recombination for our fractional IDM model by plotting the residual of the IDM power spectra with respect to Λ CDM as a function of redshift for different k (Figure 4). We may also take the linear power

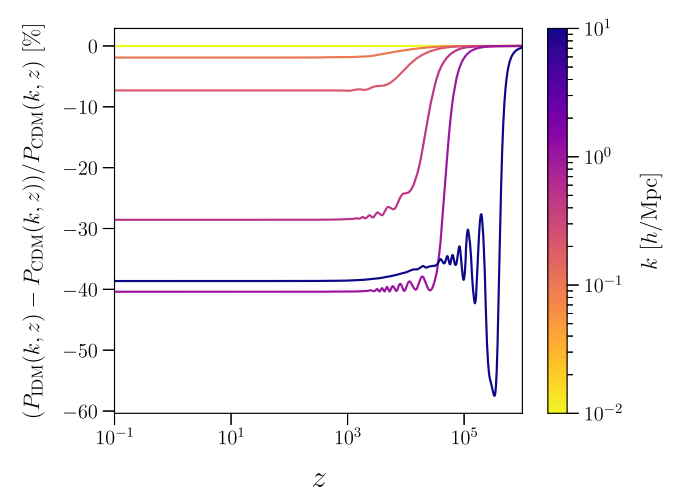


Figure 4. Residual between the power spectrum for our fractional IDM model and the power spectrum for Λ CDM as a function of redshift, for different values of k. None of the curves continue oscillating past $z\sim10^3$, indicating that there is no evolution on these scales past recombination. This means that DM-baryon interactions do not have an effect at these redshifts; if they did, the code would need to be edited to account for them. This plot is generated assuming best-fit cosmological parameters from a Planck + BOSS + DES analysis of the $f_\chi=10\%$ IDM model, with a DM particle mass $m_\chi=1$ MeV and cross section $\sigma_0=5.16\cdot10^{-26}$ cm².

spectrum generated for DM-baryon interactions and feed it into the standard nonlinear CDM pipeline implemented by CLASS-PT, without introducing any additional counterterms to the nonlinear power spectrum calculation.

Appendix B Full Cosmological Parameter Constraints

We display the full set of cosmological parameter constraints that correspond with the minimum χ^2 value in a Planck + BOSS + DES analysis of the $f_{\chi} = 10\%$, $m_{\chi} = 1$ MeV model in Table 2.

Table 2 Full Parameter Constraints for a Planck + BOSS + DES Analysis of the $f_\chi=10\%,\,m_\chi=1$ MeV Model

		Marginalized		
Parameter	Best Fit	$\mathrm{Max}\pm\sigma$	95% Lower	95% Upper
$100 \omega_{\rm b}$	2.246	$2.254^{+0.014}_{-0.015}$	2.226	2.283
ω_{DM}	0.1192	$0.12^{+0.00098}_{-0.001}$	0.118	0.1219
$100 \theta_{\rm s}$	1.042	$1.043^{+0.00045}_{-0.00054}$	1.042	1.044
$\ln(10^{10}A_{\rm s})$	3.04	$3.042^{+0.015}_{-0.015}$	3.012	3.072
$n_{\rm s}$	0.9698	$0.9725^{+0.0045}_{-0.0055}$	0.9628	0.9827
$ au_{ m reio}$	0.05215	$0.05288^{+0.0072}_{-0.0072}$	0.03864	0.06727
$10^{+26}\sigma_0$	5.163	$13.23^{+5.2}_{-6.5}$	1.55	24.57
z_{reio}	7.44	$7.491^{+0.76}_{-0.7}$	6.048	8.956
Ω_{Λ}	0.691	$0.6888^{+0.0054}_{-0.0052}$	0.6786	0.6992
Y_{He}	0.2479	$0.2479^{+6e-05}_{-6.1e-05}$	0.2478	0.248
H_0	67.88	$67.84^{+0.39}_{-0.39}$	67.1	68.6
$10^{+9}A_{\rm s}$	2.09	$2.096^{+0.032}_{-0.031}$	2.033	2.158
σ_8	0.7921	$0.7796^{+0.0068}_{-0.0094}$	0.764	0.7967
$b_1^{(1)}$	2.029	$2.013^{+0.046}_{-0.044}$	1.923	2.102
$b_2^{(1)}$	-0.6918	$-0.5745^{+0.54}_{-0.6}$	-1.679	0.558
$b_{\mathcal{G}_2}^{(1)}$	-0.5745	$-0.4302^{+0.28}_{-0.29}$	-0.9879	0.1287
$b_1^{(2)}$	2.145	$2.167^{+0.056}_{-0.056}$	2.058	2.274
$b_2^{(2)}$	-0.1907	$-0.3824^{+0.61}_{-0.67}$	-1.611	0.883
$b_{\mathcal{G}_2}^{(2)}$	-0.1638	$-0.1909_{-0.34}^{+0.33}$	-0.8453	0.4748
$b_1^{(3)}$	1.941	$1.929^{+0.043}_{-0.043}$	1.845	2.014
$b_2^{(3)}$	0.0399	$-0.1347^{+0.48}_{-0.52}$	-1.095	0.8526
$b_{\mathcal{G}_2}^{(3)}$	-0.367	$-0.3617^{+0.28}_{-0.28}$	-0.9123	0.184
$b_1^{(4)}$	1.96	$1.966^{+0.056}_{-0.055}$	1.858	2.074
$b_2^{(4)}$	-0.6163	$-0.4016^{+0.53}_{-0.58}$	-1.481	0.7131
$b_{\mathcal{G}_2}^{^{(4)}}$	-0.4559	$-0.3989^{+0.32}_{-0.32}$	-1.029	0.231

Note. The top half displays bounds for standard cosmological parameters, and the bottom half displays bounds on EFT bias parameters. "Best fit" refers to the maximum of the full posterior, while "marginalized max" refer to the maxima of the marginalized posteriors. The superscripts (1), (2), (3), and (4) of the galaxy bias parameters b_1 , b_2 , $b_{\mathcal{G}_2}$ refer to the NGC z=0.61, SGC z=0.61, NGC z=0.38, and SGC z=0.38 BOSS DR12 data chunks, respectively.

Appendix C χ^2 Statistics

Table 3 shows χ^2 values for all masses and data combinations tested in our analysis of the $f_\chi=10\%$ IDM model. We also test different fractions under a Planck + BOSS + DES analysis to see whether or not our finding is specific to the $f_\chi=10\%$ model; Table 4 shows the χ^2 statistics from these runs. We test $f_\chi=5\%$, 7.5%, 12.5%, and 15%; Figure 2 shows the effect that changing f_χ has on the linear matter power spectra of our IDM model. From Table 4, it is clear that our

 ${\bf Table~3} \\ \Delta\chi^2_{\rm min}~~{\rm Values~for~Different~Masses~and~Data~Set~Combinations~Tested~in~Our~} \\ {\rm Analysis,~for~an~Interacting~Fraction} \, f_\chi = 10\%$

		Planck +			
		Planck	BOSS	BOSS	
m_{χ}	Planck	+ BOSS	+ DES	+ DES	BOSS
100 keV	+2.48	-3.34	-4.78	-0.416	-2.398
1 MeV	+1.08	-3.48	-6.7	-0.248	-3.02
20 MeV	+1.42	-5.26	-6.42	-0.734	-1.996
100 MeV	+3.42	-3.3	-3.72	+0.034	-2.56

Note. Each $\Delta\chi^2_{\rm min}$ value is given with respect to the CDM χ^2 value for that data set.

m_{χ}	$f_{\chi} = 5\%$	$f_{\chi} = 7.5\%$	$f_{\chi} = 10\%$	$f_{\chi} = 12.5\%$	$f_{\chi} = 15\%$
100 keV	-3.66	-4.8	-4.78	-3.04	-4.54
1 MeV	-2.42	-5.08	-6.7	-4.2	-4.84
20 MeV	-2.38	-5.28	-6.42	-5.44	-5.44
100 MeV	-2.74	-2.88	-3.72	-3.88	-3.88

Note. Each $\Delta\chi^2_{\rm min}$ value is given with respect to the CDM χ^2 value for this data set combination.

fractional IDM model shows a consistent preference over CDM, regardless of DM interacting fraction.

Appendix D Posteriors

We show the full marginalized posterior distributions for all relevant parameters in our analysis of the $f_\chi=10\%$, $m_\chi=1$ MeV model in Figure 5. We show the same posterior distributions, along with the BOSS + DES posteriors, in Figure 6, and the same posteriors along with the BOSS-only posteriors in Figure 7. A CDM triangle plot with the same data combinations used in our analysis is displayed in Figure 8.

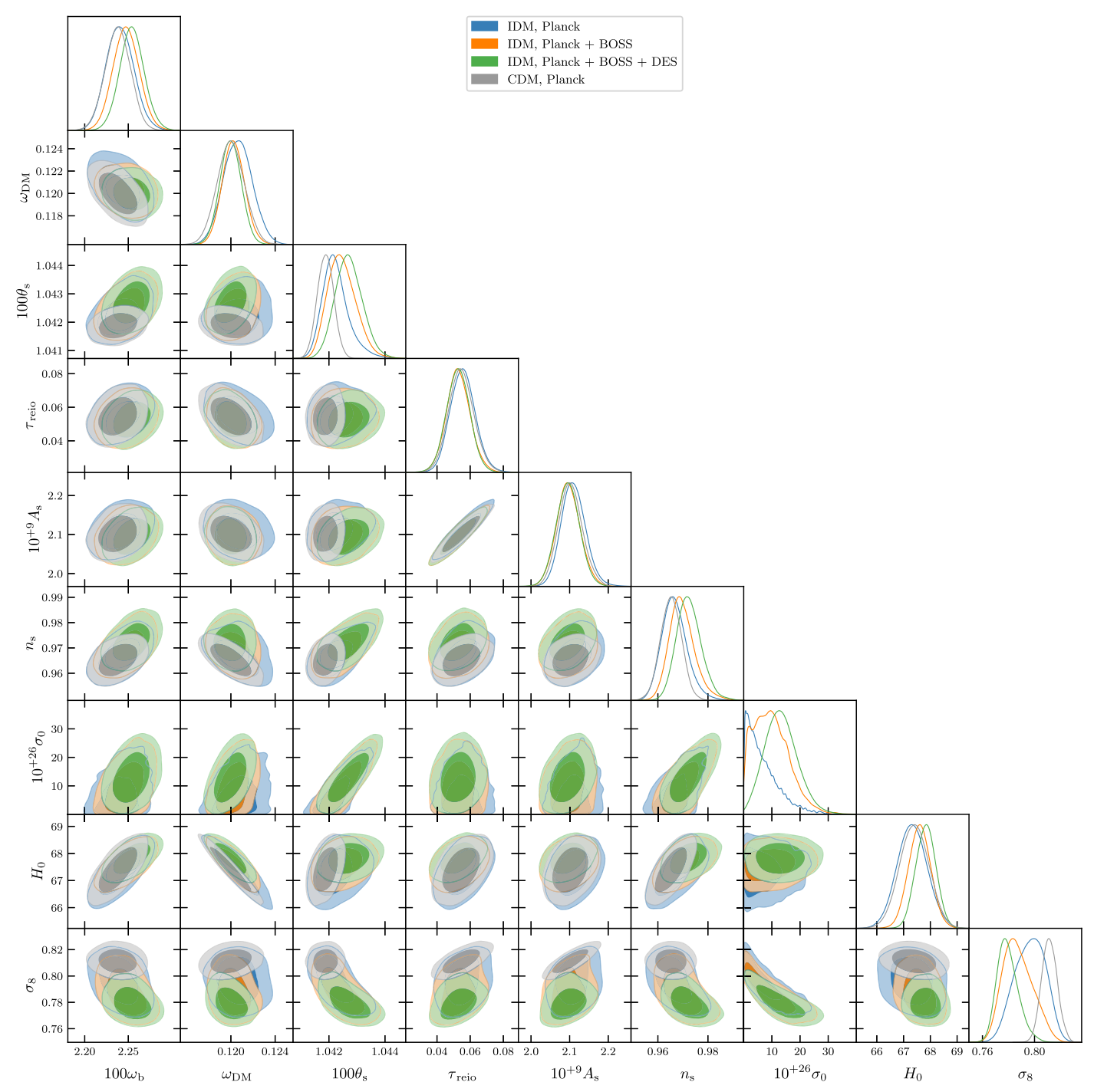


Figure 5. 68% and 95% confidence-level marginalized posterior distributions of all cosmological parameters for Λ CDM from Planck (gray) and our $m_{\chi}=1$ MeV, $f_{\chi}=10\%$ DM-baryon interacting model (colored) from different combinations of Planck, BOSS, and DES data.

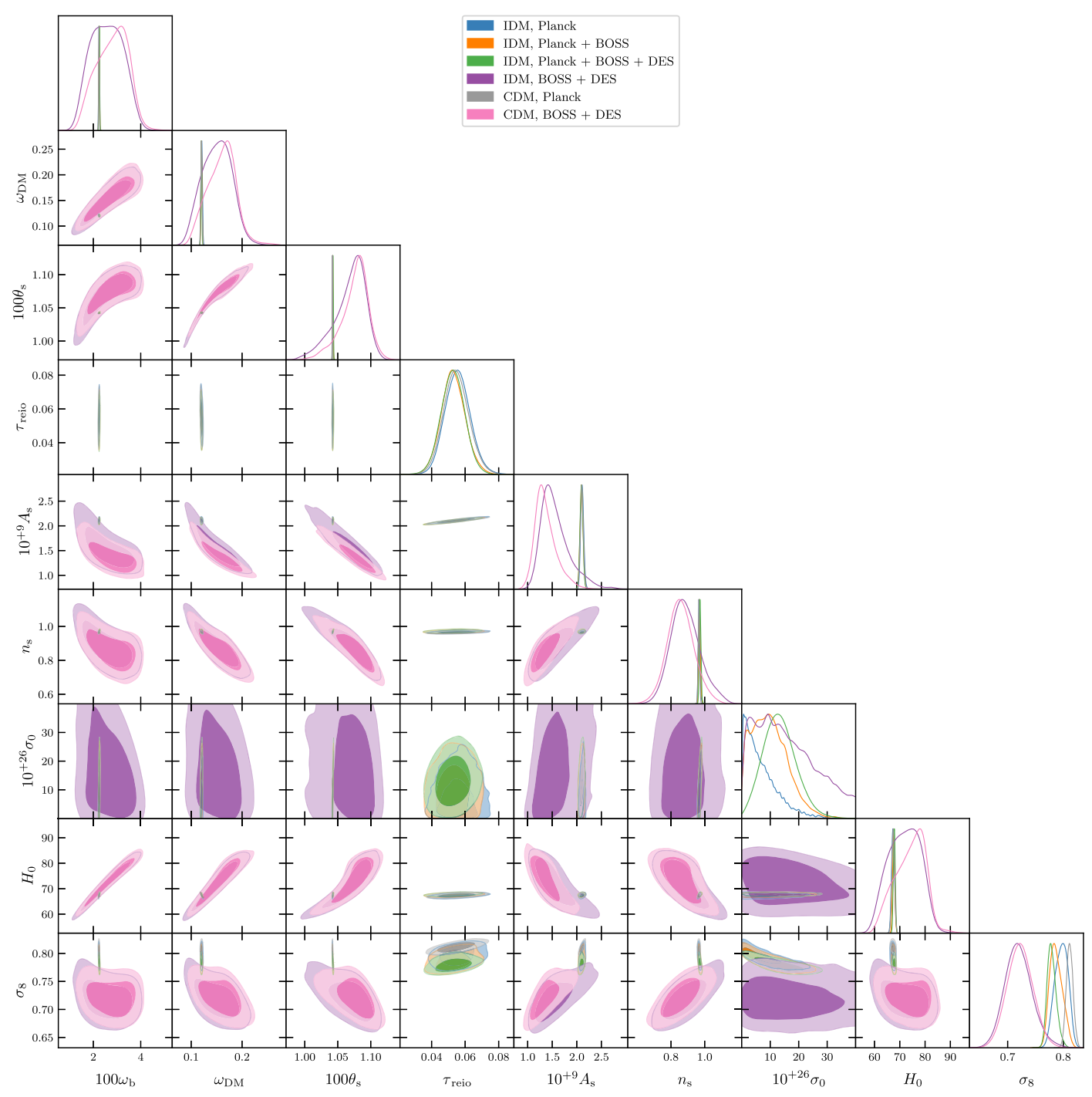


Figure 6. 68% and 95% confidence-level marginalized posterior distributions of all cosmological parameters for Λ CDM from Planck (gray) and our $m_{\chi}=1$ MeV, $f_{\chi}=10\%$ DM-baryon interacting model (colored) from different combinations of Planck, BOSS, and DES data. Same as Figure 5 but with posteriors for BOSS + DES added.

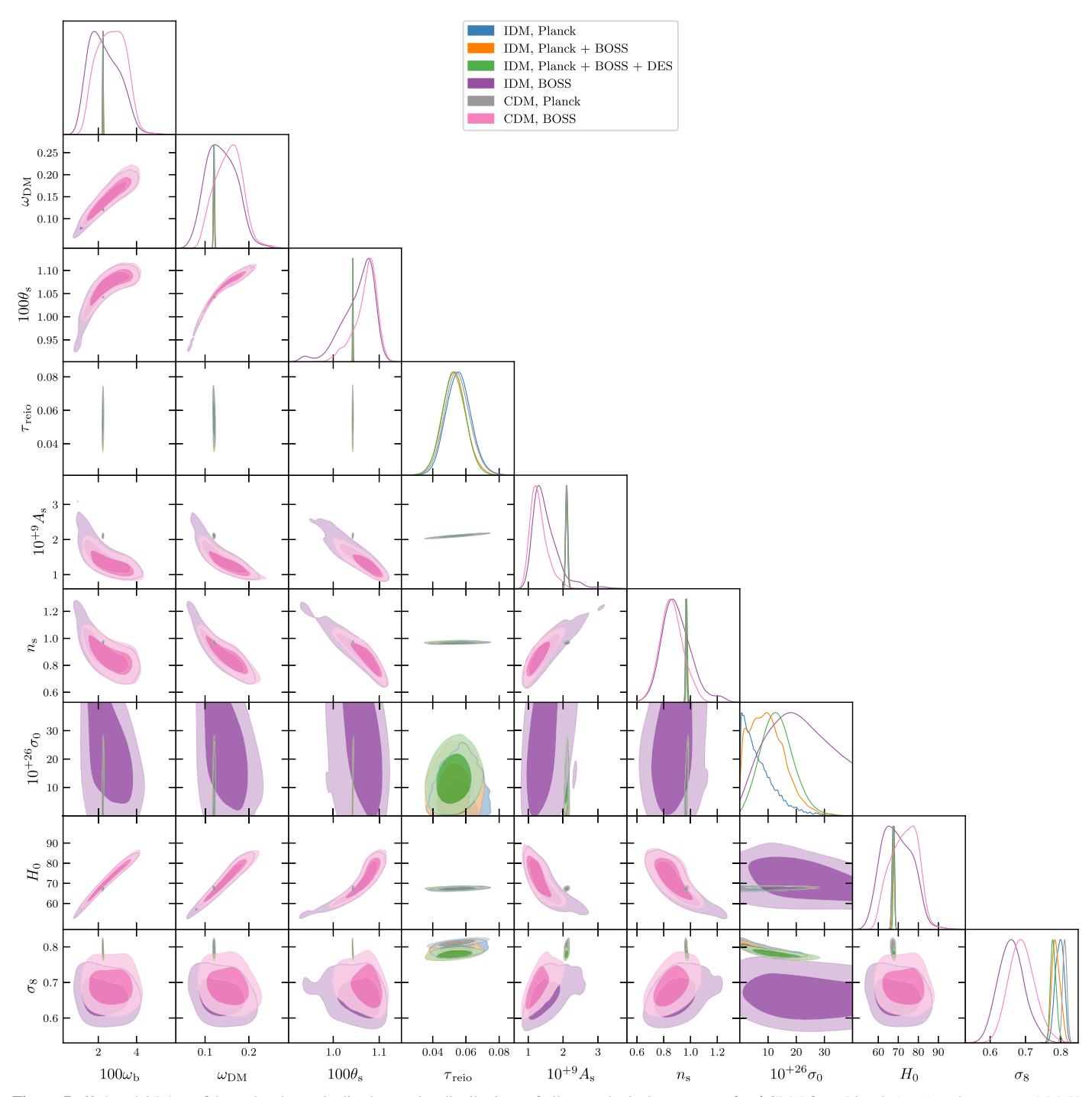


Figure 7. 68% and 95% confidence-level marginalized posterior distributions of all cosmological parameters for Λ CDM from Planck (gray) and our $m_{\chi}=1$ MeV, $f_{\chi}=10\%$ DM-baryon interacting model (colored) from different combinations of Planck, BOSS, and DES data. Same as Figure 5 but with posteriors for BOSS-only analyses.

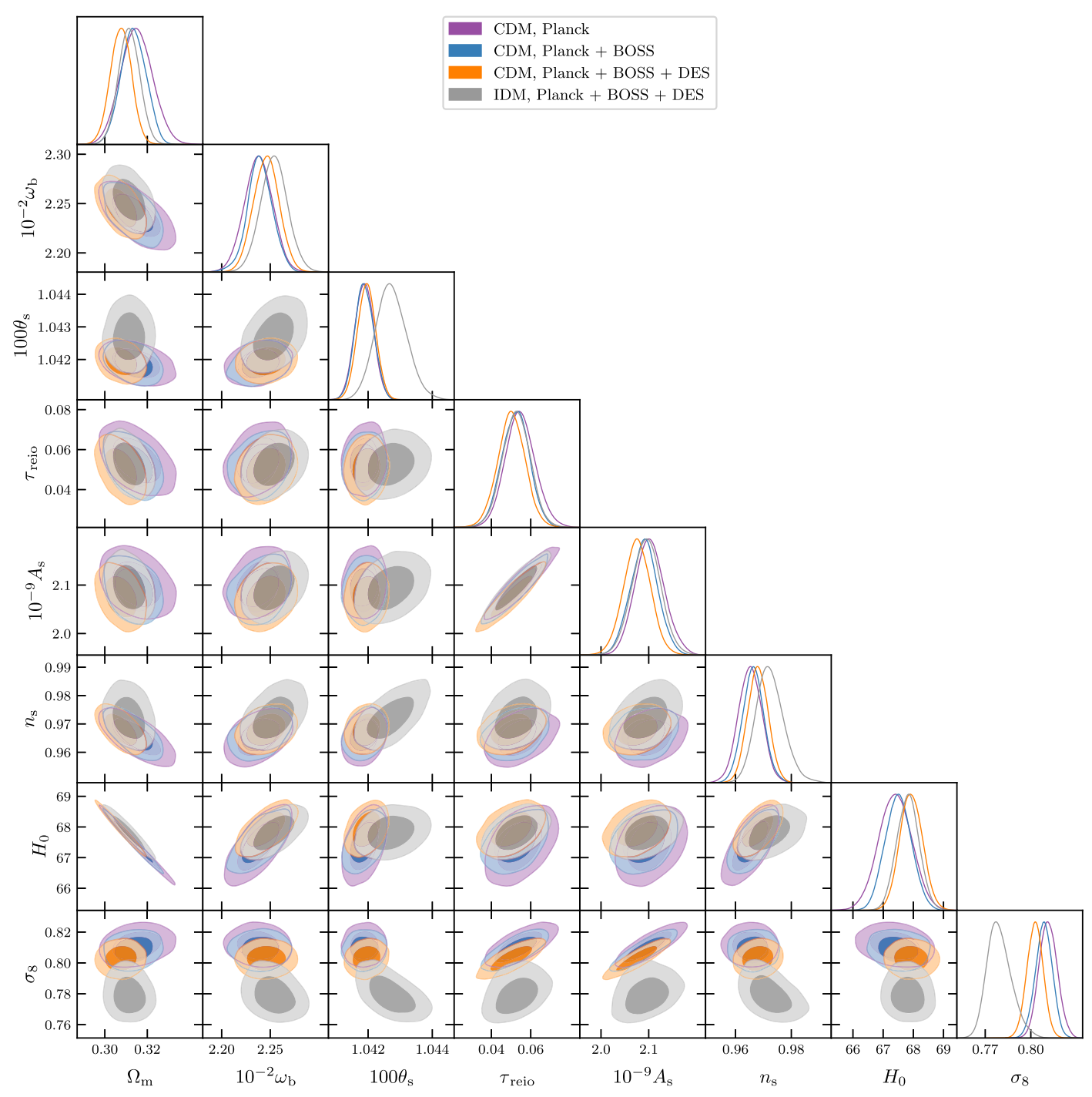


Figure 8. 68% and 95% confidence-level marginalized posterior distributions of all cosmological parameters for our IDM model from a Planck + BOSS + DES analysis (gray) and for Λ CDM (colored) from different combinations of Planck, BOSS, and DES data.

Appendix E Log Prior Results

To assess prior dependence, we run a Planck + BOSS + DES analysis of the $f_\chi=10\%,\ m_\chi=1$ MeV model with a log prior on σ_0 . We choose the range of the log prior to be [-30, -23]. Table 5 shows marginalized limits on σ_0 and S_8 from this analysis, along with the $\Delta\chi^2_{\rm min}$ with respect to $\Lambda{\rm CDM}$. We

display 68% and 95% confidence-level marginalized posterior distributions of all cosmological parameters for this analysis in Figure 9. The log prior finds $\Delta\chi^2_{\rm min}=-5.6$, which still indicates a nonnegligible $>\!\!2\sigma$ preference for our IDM model over CDM. We therefore state that our IDM model shows consistent preference over $\Lambda \rm CDM$ regardless of the prior choice.

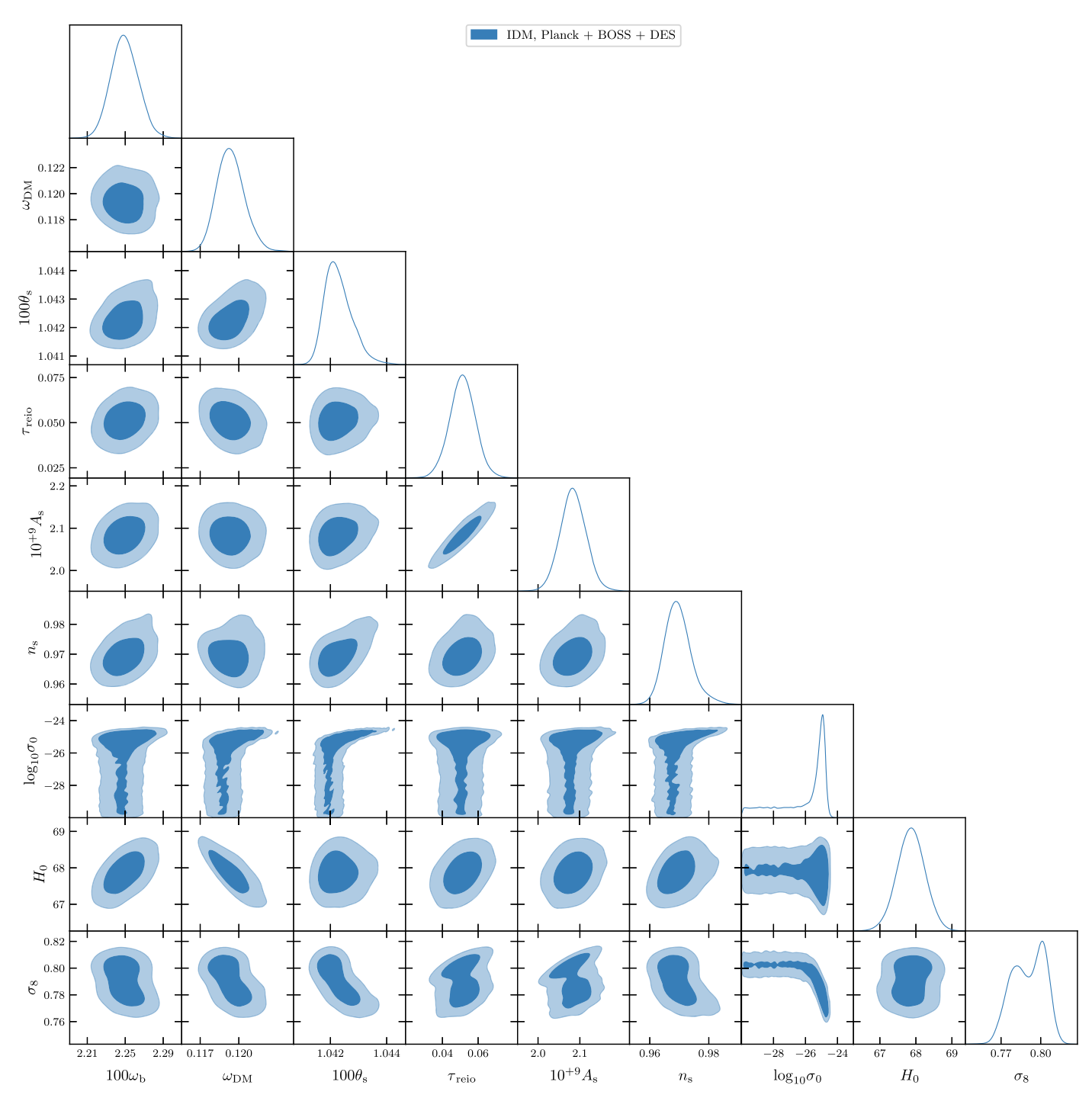


Figure 9. 68% and 95% confidence-level marginalized posterior distributions of all cosmological parameters for our $m_{\chi} = 1$ MeV, $f_{\chi} = 10\%$ DM-baryon interacting model under a Planck, BOSS, and DES analysis and a log prior on σ_0 .

Table 5

Maximum of the Marginalized Posterior (Maximum of the Full Posterior, or the Best-fit Value) and $\pm 68\%$ Confidence Level Uncertainties for σ_0 and S_8 under a Planck + BOSS + DES Analysis of Our Fractional IDM Model with a Log Prior on σ_0 , Compared to ΛCDM .

Model	ΛCDM, Planck + BOSS + DES	IDM, Planck + BOSS + DES
$\frac{\log_{10}(\sigma_0/\text{cm}^2)}{S_8}$	$$ $0.813 (0.813) \pm 0.009$	$-26.2 (-24.96)^{+1.6}_{-0.43}$ $0.803 (0.795)^{+0.014}_{-0.012}$
$\Delta\chi^2_{ m min}$		-5.6

Note. The last row shows the difference in χ^2 with respect to Λ CDM. All IDM values are for $m_\chi = 1$ MeV, $f_\chi = 10\%$.

ORCID iDs

Adam He https://orcid.org/0000-0003-2501-5842

References

```
Aalseth, C. E., Barbeau, P. S., Colaresi, J., et al. 2013, PhRvD, 88, 012002
Abazajian, K. N., Adshead, P., Ahmed, Z., et al. 2016, arXiv:1610.02743
Abbott, T., Aguena, M., Alarcon, A., et al. 2022, PhRvD, 105, 023520
Abdalla, E., Abellán, G. F., Aboubrahim, A., et al. 2022, JHEAp, 34, 49
Ade, P., Aguirre, J., Ahmed, Z., et al. 2019, JCAP, 02, 056
Aghamousa, A., Aguilar, J., Ahlen, S., et al. 2016, arXiv:1611.00036
Aghanim, N., Akrami, Y., Ashdown, M., et al. 2020a, A&A, 641, A5
Aghanim, N., Akrami, Y., Ashdown, M., et al. 2020b, A&A, 641, A8
Aghanim, N., Akrami, Y., Ashdown, M., et al. 2020c, A&A, 641, A6
Agnes, P., Albuquerque, I. F. M., Alexander, T., et al. 2018, PhRvL, 121,
Agnese, R., Aramaki, T., Arnquist, I., et al. 2018, PhRvL, 120, 061802
Agnese, R., Anderson, A. J., Aramaki, T., et al. 2016, PhRvL, 116, 071301
Aguilar-Arevalo, A., Amidei, D., Baxter, D., et al. 2019, PhRvL, 123, 181802
Aiola, S., Calabrese, E., Maurin, L., et al. 2020, JCAP, 12, 047
Aiola, S., Akrami, Y., Basu, K., et al. 2022, arXiv:2203.05728
Akerib, D., Alsum, S., Araújo, H., et al. 2017, PhRvL, 118, 021303
Akerib, D. S., Cushman, P. B., Dahl, C. E., et al. 2022, arXiv:2203.08084
Alam, S., Ata, M., Bailey, S., et al. 2017, MNRAS, 470, 2617
Alam, S., Aubert, M., Avila, S., et al. 2021, PhRvD, 103, 083533
Amole, C., Ardid, M., Arnquist, I., et al. 2017, PhRvL, 118, 251301
Amole, C., Ardid, M., Arnquist, I. J., et al. 2019, PhRvD, 100, 022001
Amon, A., & Efstathiou, G. 2022, MNRAS, 516, 5355
Amon, A., Gruen, D., Troxel, M., et al. 2022a, PhRvD, 105, 023514
Amon, A., Robertson, N. C., Miyatake, H., et al. 2022b, MNRAS, 518, 477
An, R., Gluscevic, V., Calabrese, E., & Hill, J. C. 2022, JCAP, 2022, 002
Angle, J., Aprile, E., Arneodo, F., et al. 2008, PhRvL, 100, 021303
Angloher, G., Bauer, P., Bento, A., et al. 2017, EPJC, 77, 637
Angloher, G., Bento, A., Bucci, C., et al. 2016, EPJC, 76, 25
Aprile, E., Aalbers, J., Agostini, F., et al. 2018, PhRvL, 121, 111302
Asgari, M., Lin, C., Joachimi, B., et al. 2021, A&A, 645, A104
Audren, B., Lesgourgues, J., Benabed, K., & Prunet, S. 2013, JCAP, 1302, 001
Battaglieri, M., Belloni, A., Chou, A., et al. 2017, arXiv:1707.04591
Baumann, D., Nicolis, A., Senatore, L., & Zaldarriaga, M. 2012, JCAP, 07, 051
Becker, N., Hooper, D. C., Kahlhoefer, F., Lesgourgues, J., & Schöneberg, N.
   2021, JCAP, 2021, 019
Benson, B. A., Ade, P. A. R., Ahmed, Z., et al. 2014, Proc. SPIE, 9153,
  91531P
Bernal, J. L., Verde, L., & Riess, A. G. 2016, JCAP, 2016, 019
Bertone, G., Hooper, D., & Silk, J. 2005, PhR, 405, 279
Boddy, K. K., & Gluscevic, V. 2018, PhRvD, 98, 083510
Boddy, K. K., Gluscevic, V., Poulin, V., et al. 2018, PhRvD, 98, 123506
Bœhm, C., Fayet, P., & Schaeffer, R. 2001, PhLB, 518, 8
Boehm, C., & Schaeffer, R. 2005, A&A, 438, 419
Brinckmann, T., & Lesgourgues, J. 2019, PDU, 24, 100260
Brout, D., Scolnic, D., Popovic, B., et al. 2022, ApJ, 938, 110
Buen-Abad, M. A., Essig, R., McKeen, D., & Zhong, Y.-M. 2022, PhR, 961, 1
```

```
Simonović, M. 2023, PDU, 40, 101193
Carrasco, J. J. M., Hertzberg, M. P., & Senatore, L. 2012, JHEP, 2012, 82
Chabanier, S., Millea, M., & Palanque-Delabrouille, N. 2019, MNRAS,
  489 2247
Chaves-Montero, J., Angulo, R. E., & Contreras, S. 2023, MNRAS, 521,
Chen, S.-F., Vlah, Z., & White, M. 2022, JCAP, 02, 008
Chudaykin, A., Dolgikh, K., & Ivanov, M. M. 2021, PhRvD, 103, 023507
Chudaykin, A., & Ivanov, M. M. 2019, JCAP, 11, 034
Chudaykin, A., & Ivanov, M. M. 2023, PhRvD, 107, 043518
Chudaykin, A., Ivanov, M. M., Philcox, O. H., & Simonović, M. 2020,
    PhRvD, 102, 063533
Cushman, P., Galbiati, C., McKinsey, D. N., et al. 2013, arXiv:1310.8327
DES Collaboration, Abbott, T. M. C., Aguena, M., et al. 2023, PhRvD, 107,
Drlica-Wagner, A., Mao, Y.-Y., Adhikari, S., et al. 2019, arXiv:1902.01055
Dvorkin, C., Blum, K., & Kamionkowski, M. 2014, PhRvD, 89, 023519
Gluscevic, V., Ali-Haimoud, Y., Bechtol, K., et al. 2019, BAAS, 51, 134
Gluscevic, V., & Boddy, K. K. 2018, PhRvL, 121, 081301
Gluscevic, V., & Peter, A. H. 2014, JCAP, 2014, 040
Goldstein, S., Hill, J. C., Iršič, V., & Sherwin, B. D. 2023, arXiv:2303.00746
Hikage, C., Oguri, M., Hamana, T., et al. 2019, PASJ, 71, 43
Hill, J. C., McDonough, E., Toomey, M. W., & Alexander, S. 2020, PhRvD,
  102. 043507
Hooper, D. C., Schöneberg, N., Murgia, R., et al. 2022, JCAP, 2022, 032
Ivanov, M. M. 2021, PhRvD, 104, 103514
Ivanov, M. M. 2022, arXiv:2212.08488
Ivanov, M. M., McDonough, E., Hill, J. C., et al. 2020a, PhRvD, 102, 103502
Ivanov, M. M., Philcox, O. H. E., Nishimichi, T., et al. 2022a, PhRvD, 105,
Ivanov, M. M., Philcox, O. H. E., Simonović, M., et al. 2022b, PhRvD, 105,
  043531
Ivanov, M. M., Simonović, M., & Zaldarriaga, M. 2020b, JCAP, 2020, 042
Ivanov, M. M., Simonović, M., & Zaldarriaga, M. 2020c, PhRvD, 101, 083504
Ivezić, Ž., Kahn, S. M., Tyson, J. A., et al. 2019, ApJ, 873, 111
Kim, Y., Lindner, A., & Semertzidis, Y. K. 2017, 12th "Patras" Workshop on
   Axions, WIMPs and WISPs, PATRAS 2016, DESY-PRO (Hamburg:
Leauthaud, A., Saito, S., Hilbert, S., et al. 2017, MNRAS, 467, 3024
Lewin, J. D., & Smith, P. F. 1996, APh, 6, 87
Li, Z., An, R., Gluscevic, V., et al. 2023, JCAP, 02, 046
Maamari, K., Gluscevic, V., Boddy, K. K., Nadler, E. O., & Wechsler, R. H.
  2021, ApJL, 907, L46
Nadler, E., Drlica-Wagner, A., Bechtol, K., et al. 2021, PhRvL, 126, 091101
Nadler, E. O., Gluscevic, V., Boddy, K. K., & Wechsler, R. H. 2019, ApJ,
  878, L32
Nguyen, D. V., Sarnaaik, D., Boddy, K. K., Nadler, E. O., & Gluscevic, V.
  2021, PhRvD, 104, 103521
Philcox, O. H. E., & Ivanov, M. M. 2022, PhRvD, 105, 043517
Philcox, O. H. E., Ivanov, M. M., Simonović, M., & Zaldarriaga, M. 2020,
   JCAP, 05, 032
Poulin, V., Bernal, J. L., Kovetz, E., & Kamionkowski, M. 2023, PhRvD, 107,
   123538
Preston, C., Amon, A., & Efstathiou, G. 2023, arXiv:2305.09827
Qu, F. J., Sherwin, B. D., Madhavacheril, M. S., et al. 2023, arXiv:2304.05202
Rogers, K. K., Dvorkin, C., & Peiris, H. V. 2022, PhRvL, 128, 171301
Rogers, K. K., Hložek, R., Laguë, A., et al. 2023, JCAP, 06, 023
Sailer, N., Castorina, E., Ferraro, S., & White, M. 2021, JCAP, 12, 049
Sigurdson, K., Doran, M., Kurylov, A., Caldwell, R. R., & Kamionkowski, M.
  2004, PhRvD, 70, 083501
Slatyer, T. R., & Wu, C.-L. 2018, PhRvD, 98, 023013
Tseliakhovich, D., & Hirata, C. 2010, PhRvD, 82, 083520
Valentino, E. D., Anchordoqui, L. A., Özgür Akarsu, et al. 2021a, APh, 131,
  102604
Valentino, E. D., Anchordoqui, L. A., Özgür Akarsu, et al. 2021b, APh, 131,
Xu, W. L., Dvorkin, C., & Chael, A. 2018, PhRvD, 97, 103530
Xu, X., & Farrar, G. R. 2021, arXiv:2112.00707
Ye, G., Zhang, J., & Piao, Y.-S. 2021, arXiv:2107.13391
Zhang, P., D'Amico, G., Senatore, L., Zhao, C., & Cai, Y. 2022, JCAP,
  02, 036
```

Cabass, G., Ivanov, M. M., Lewandowski, M., Mirbabayi, M., &